ENHANCED CLASSIFICATION-BASED VESSEL TRACKING USING VESSEL MODELS AND HOUGH TRANSFORM

A. Giani*, E. Grisan*, and A. Ruggeri*

* Department of Information Engineering, University of Padova, Italy

giani@dei.unipd.it

Abstract: Analysis of blood vessels in images of retinal fundus is an important and non-invasive procedure for the diagnosis of many diseases. To derive useful clinical features, such as vessel diameter and tortuosity, an accurate segmentation of the vessel network has to be performed. In this paper we describe a novel classification-based tracking algorithm that enhances the performance of classification based techniques by extending the observation window upon which classification takes place, and enforces robust estimate of the local geometry of the vessel.

Introduction

Analysis of blood vessels in images of retinal fundus is an important and non-invasive procedure for the diagnosis of many diseases [1,2]. To derive useful clinical features, such as vessel diameter and tortuosity, an accurate segmentation of the vessel network has to be performed.

The tracking-based segmentation methods proposed in the literature start from a set of seed points and proceed along the corresponding vessels, using either 2-D matched filters [3] or classification techniques (vessel or non vessel pixels) based on vessel profiles [4]. Seed points can be initially found from easily recognizable areas of the image (e.g. the optic disc [4]) but this approach may fail to track peripheral and low-contrast vessels. A more principled approach is sparse tracking [5], where seeds are found over the whole image. This in turn requires a joining algorithm that connects segments resulting from separate tracking of the same vessel. Compared to global techniques, that process the whole image by convoluting it with a pyramidal set of 2D Gaussian templates [6], tracking has obvious advantages in terms of computational efficiency. Furthermore, tracking techniques also provide a way of locally adapting vessel segmentation to image features, since an estimate of local luminosity can be calculated as tracking progresses, although global techniques can be provided with adaptation as a post-processing stage of the convolution result [7]. Also, it should be noted that, in order to recover useful clinical information, vessel tracking must be necessarily applied to produce a geometrical model of the vessel.

A problem that may affect classification methods is that small vessels and background are often non-separable in grayscale space. This issue is particularly critical for profile-based methods, where classification is performed over one or few cross-sections of the vessel under exam [4]. Even apparently well-defined vessels may cause the tracking to halt wherever noise or natural texture (pigmentation) of the free fundus cause local drop of the contrast or lack of separability. Computationally-demanding matched filters tackle this problem trading-off computational cost with sensibility, as the whole grayscale dynamics of the vessel profile are considered over several consecutive profiles convoluted with a Gaussian-shaped kernel (figure 1).

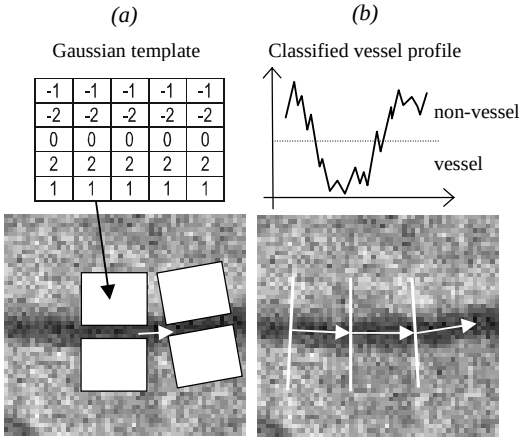

Figure 1. Matched filters based (a) and profile classification based (b) vessel tracking.

Methods

In this paper we describe a novel classification-based tracking algorithm that enhances the performance of these techniques by extending the observation window upon which classification takes place, and enforcing robust estimate of the local geometry of the vessel. The rationale is to recover that depth information typically neglected in profile-based methods. The key features of the proposed algorithm are:

- A seed finding procedure that seeks for the two goals of providing a satisfactory initial set of seeds, and allowing tracking to proceed whenever changes in vessel topology (e.g. bifurcations, branching, or local "holes" in the vessel) and lack of contrast/separation cause the current tracking to halt
- Robust estimate of vessel borders based on the Hough Transform (HT) that provides the tracking

ISSN: 1727-1983

with an estimate of local caliber and direction, so that the following tracking point can be determined

- Local adaptation to contrast variations with variable computational complexity, yielding fast adaptation in normal cases and more sophisticated adaptation when the simpler technique fails.

Seed finding procedure

An initial seed-finding algorithm, based on simple edge detection over a regular grid, is run. The keystone of seed finding is bubble search procedure we previously developed [5] that estimates caliber d and direction θ of each candidate seed by classifying an annular region (seed support) around the candidate seed. Inner and outer radii of the region are proportional to the distance between the two edges found. Since no estimate of local contrast is available at this stage, vessel-non vessel binary classification is achieved using Fuzzy C-Means (FCM) clustering [4]. The resulting estimate is strengthened with respects to the algorithm currently found in literature by checking geometrical consistency of the estimated caliber d and direction θ with the initial edges distance d' given an empirical tolerance Δd (Figure 2)

$$d = \in \left[d' \cos\theta - \Delta d \, , d' \cos\theta + \Delta d \right] \qquad (1)$$

If (1) is satisfied the seed is considered for further processing.

Robust Vessel Estimate

Once a valid seed is determined, tracking main procedure is started. Under the assumption of the presence of a vessel, two vessel borders should be found within a rectangular region (vessel support) oriented according to the previously found direction (prior information) and including an approximately straight section of the vessel. In order to allow automatic contrast detection and classification, enough background should be included in the support. Under these guidelines, empirical observations suggested us to have a support that is 3d wide and d deep along vessel direction, expecting vessel curvature to be locally negligible.

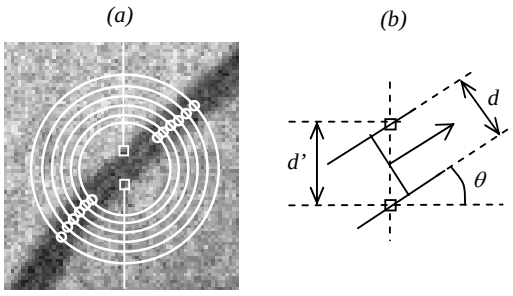

Figure 2: Edge detection (squares) and bubble search (circles) (a). Geometrical consistency of the estimated seed with the initial edges.

Vessel borders are therefore modeled as straight lines Λ:{ρ,ϕ} described in terms of distance ρ from the axis origin and angle ϕ (figure 3). Line detection is achieved by using robust Hough Transform (HT) [8] that uses a continuous voting kernel

$$K_{\rho,\phi}(\xi) = \begin{cases} 1 - 2\frac{\xi^2}{w^2} + \frac{\xi^4}{w^4} & |\xi| \le w \\ 0 & otherwise \end{cases} \qquad (2)$$

where ξ is the distance of the border point under investigation from the considered border model Λ and w is the minimum distance from the model in order for a border point to contribute (vote) to the HT accumulator in ρ,ϕ. Equation (2) is continuous and differentiable and yields greater outlier rejection and robustness compared to the ordinary top-hat voting kernel found in standard HT [9].

The computational complexity of HT, which seeks for lines by finding maxima in the 2-dimensional accumulator space, is reduced by using the previously calculated border vessels as a prior estimate (with some uncertainty) for the two intercepts in the vessel support. The angular drift (direction change) is also limited within a maximum expected curvature. In other words, given the previously tracked borders, not all the possible new borders in the support are accepted. Therefore, the maxima finding problem is reduced to a quasi-1D problem (Figure 4)

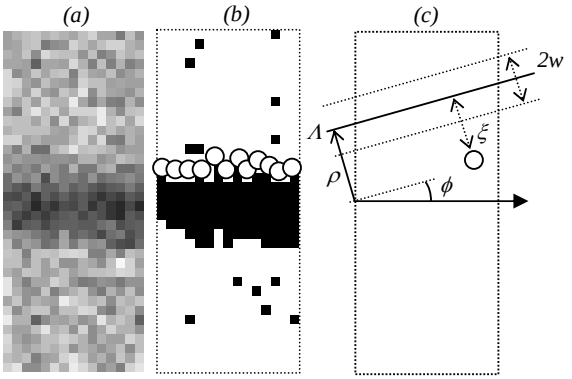

Figure 3: Hough Transform (top vessel border). Vessel support (a) is thresholded and candidate border points (circles) are found (b) compatible with prior tracking. Any candidate border line Λ is compared against the number of points that significantly vote for it (c).

If two (and only two) vessel border lines are found, consistent with the current vessel caliber and direction, new vessel center, diameter and direction are estimated and the support is moved further along the newly estimated vessel direction. If the pattern of lines found by HT suggests a change of vessel shape (e.g. bifurcation) or is not consistent with a vessel structure (e.g. HT does not detect one of the borders), bubble search is reapplied in the attempt to find new seeds. The whole procedure is iterated until no new seeds are found.

ISSN: 1727-1983

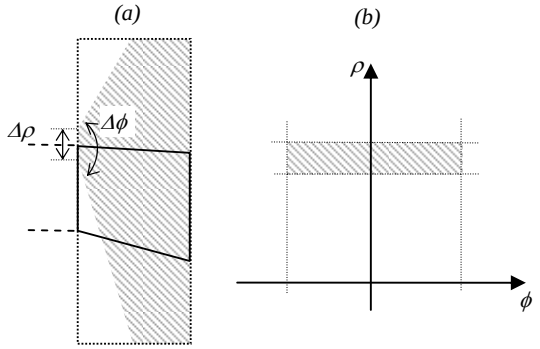

Figure 4. Within the vessel support (dotted), the top border must lay in the shaded gray area only, determined from the previously tracked border (dashed) (a). Therefore, the HT accumulator is reduced to a narrow strip (b).

Adaptive Threshold

In absence of prior information, the classification threshold is initially determined by FCM and then updated to adapt to local luminance and contrast, using a faster estimate. Once two vessel borders have been determined, the classification threshold to be used in the next step is rapidly calculated as

$$th = 0.6 \cdot Lint + 0.4 \cdot \left(Lext_u + Lext_l \right) / 2 \qquad (3)$$

where, being $p(x, y)$ the pixel value in the vessel support and $Aint$, $Aext_u$, $Aext_l$ respectively the internal, upper external and lower external parts of the support with respects to the estimated vessel borders (figure 5), we define the internal, upper external and lower external average luminosities as

$$\begin{aligned} Lint &= \left\langle p(x, y) \,\middle|\, x, y \in Aint \right\rangle \\ Lext_u &= \left\langle p(x, y) \,\middle|\, x, y \in Aext_u \right\rangle \\ Lext_l &= \left\langle p(x, y) \,\middle|\, x, y \in Aext_l \right\rangle \end{aligned} \qquad (4)$$

Note that the algebra in (3) has been left redundant to separate and underline the empirical weighting of internal and external luminances. By applying (3), we expect to gather evidence for the estimated geometry, since low contrast betrays insufficient grayscale separation between pixels supposed to belong to the vessel and those supposed to belong to the background. In order to ensure enough stability and outliers rejection (e.g. neighboring vessels), the averages are calculated over two previously tracked sections and averages excessively departing from the corresponding priors are excluded from (3). Still, the threshold estimate may become unstable if large errors occur in border slopes, causing an excessive number of background pixels to be misclassified as belonging to the vessel, or vice-versa (Figure 5). This in turn starts an "avalanche effect" that leads to unbounded divergence/collapsing convergence of the vessel borders. When this diverging/collapsing pattern is detected over two tracking steps, tracking is moved back and a slower but more robust FCM-based threshold is applied. In other words, FCM is applied whenever the estimated vessel departs from the simpler constant-caliber model. The rationale is to optimize the computational effort, preferring faster average-based threshold estimate whenever is possible. Contrast also provides a termination condition if contrast falls below a given value.

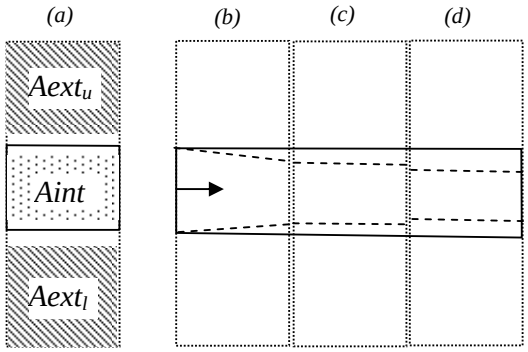

Figure 5. Threshold adaptation: internal (dotted) and upper/lower external areas (slanted) (a). A large error in border estimate (b) may cause threshold over-estimate. This in turn may cause caliber under-estimate (c) and collapse as tracking proceeds (d).

Materials

A set of 40 fundus images is considered for testing the algorithm, made of 20 normal (healthy) cases and 20 pathological cases. Luminance and contrast drifts are removed using an ISO-illumination method we developed [10]. This pre-processing step also ensures uniform inter-images contrast and luminosity, therefore ensuring luminance and contrast invariance. Images are hand-labeled by human experts in order to provide ground truth to be compared against the results.

Results and Discussion

Results show 92% average sensitivity and average 6.6% of false vessels detected (table 1), with satisfactory uniform performance over the images (figure 6, 7).

Our approach combines a robust, model-based classification technique with some principles of matched filters methods. Vessel borders are estimated using fast and robust adaptive classification. The vessel is then validated according to its contrast value, which can be seen as the response of a single square-window matched filter. The rationale is then to minimize computational complexity (matched filters) by separating the geometrical problem (vessel geometry) from the validation problem (grayscale consistency). The lack of robustness typical of classification methods is tackled using a novel algorithm based on a combination of prior information, Hough Transform, adaptive contrast and bubble search.

ISSN: 1727-1983

Table 1: overall results: sensitivity and false detections (mean/variance).

	healthy	pathological
sensitivity %	94/2	91/5.6
false vases %	6.9/6.3	6.4/9

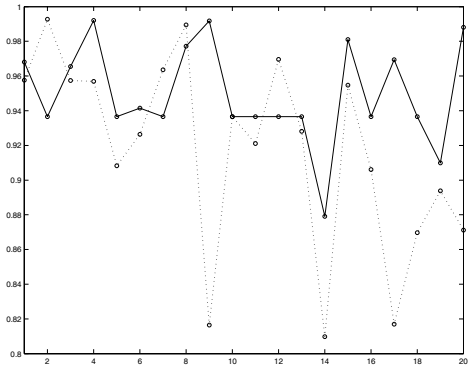

Figure 6. Normalized sensitivity over the sets of 20 healthy (full) and 20 pathological (dotted) images.

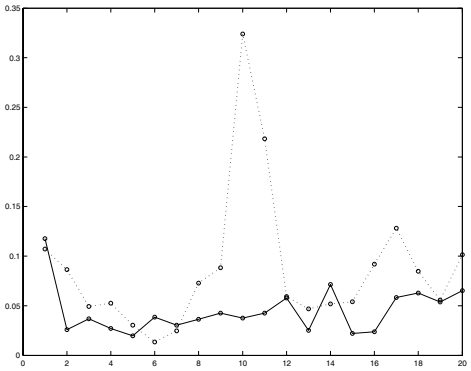

Figure 7. Normalized number of false vessels over the sets of 20 healthy (full) and 20 pathological (dotted) images.

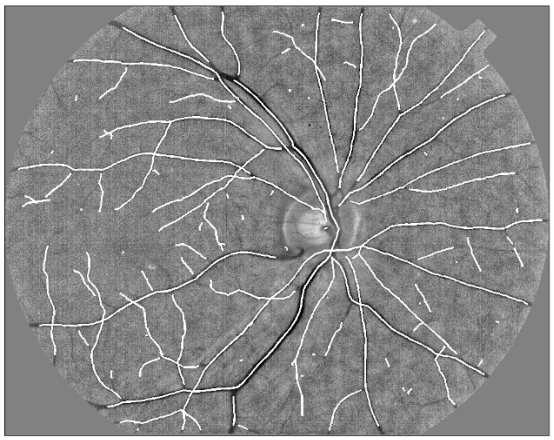

Figure 8. Tracking result on a test image.

References

[1] LEUNG H. et Al. "Relationships between Age, Blood Pressure, and Retinal Vessel Diameters in an Older Population" *Investigative Ophthalmology & Visual Science*, Vol. 44, No. 7, 2003.

[2] STANTON A. V. et Al. "Vascular network changes in the retina with age and hypertension," *Journal of Hypertension*, Vol. 13, pp. 1724–1728, 1995.

[3] CHUTATAPE O., ZHENG L., KRISHNAN S. M., "Retinal blood vessel detection and tracking by matched gaussian and Kalman filters," in *Proc. 20th of IEEE EMBS International Conference*, pp. 3144–3149, 1998.

[4] TOLIAS Y. A. PANAS S. M., "A fuzzy vessel tracking algorithm for retinal images based on fuzzy clustering," *IEEE Transactions on Medical Imaging*, Vol. 17, No. 2, pp. 263–273, 1998.

[5] GRISAN E., PESCE A., GIANI A., FORACCHIA M., RUGGERI A.: "A new tracking system for the robust extraction of retinal vessel structure", in *Proc. 26th IEEE EMBS International Conference*, pp. 1620-1623, 2004.

[6] CHAUDHURI S., CHATTERJEE S., KATZ N., NELSON M., GOLDBAUM M. "Detection of Blood Vessels in Retinal Images Using Two-Dimensional Matched Filters" *IEEE Transactions on Medical Imaging*, Vol. 8, No. 3, pp. 263-269, 1989.

[7] HOOVER A., KOUZNESTOVA V., GOLDBAUM M. "Locating blood vessels in retinal images by piece-wise threshold probing of a matched filter response," *IEEE Transactions on Medical Imaging*, Vol. 19, No. 3, pp. 203–210, 2000.

[8] PALMER P. L., KITTLER J., PETROU M. "An Optimizing Line Finder Using a Hough Transform Algorithm" *Computer Vision and Image Understanding*, Vol. 67, No. 1, pp. 1–23, 1997.

[9] DUDA R. D., P. HART E., "Use of the Hough transform to detect lines and curves in pictures", *Comm. Assoc. Comput. Mach.*, Vol. 15, pp. 11–15, 1972.

[10] FORACCHIA M., GRISAN E., RUGGERI A., "Luminosity and contrast normalization in retinal images," *Medical Image Analysis*, Vol. 2, pp. 179–190, 2005.